*Marine Geology*, 116 (1994) 399–418
Elsevier Science B.V., Amsterdam



# Non-annual laminations and expansion of anoxic basin-floor conditions in Santa Monica Basin, California Borderland, over the past four centuries

Christopher J. Christensen[1], Donn S. Gorsline[2], Douglas E. Hammond and Steven P. Lund
*Department of Geological Sciences, University of Southern California, Los Angeles, CA 90089-0740, USA*

(Received August 3, 1992; revision accepted September 8, 1993)

ABSTRACT

Christensen, C.J., Gorsline, D.S., Hammond, D.E. and Lund, S.P., 1994. Non-annual laminations and expansion of anoxic basin-floor conditions in Santa Monica Basin, California Borderland, over the past four centuries. In: M.I. Scranton (Editor), Variability in Anoxic Systems. *Mar. Geol.*, 116: 399–418.

Sediments from box cores in the deep portion of Santa Monica Basin have been examined by X-radiography, and the upper 10–20 cm are characterized by laminations 1–5 mm in thickness. Age dating of 9 cores by $^{210}$Pb analysis has shown that accumulation rates on the central basin floor have been remarkably constant during the past century, averaging $16.0 \pm 0.4$ mg/cm$^2$/yr. Densitometer analysis of the X-radiography films from 7 cores and spectral analysis of the resulting time series indicates that most lamination couplets have a periodicity in the 3–7 year range, a range matching that of the El Niño-Southern Oscillation periodicity. The median periodicity appears to have decreased slightly during the past 3 centuries, from 7.0 years during 200–300 yrs B.P. to 5.2 yrs during 0–100 yrs B.P. This trend could be due to a decreasing sedimentation rate, an increasing forcing frequency, or an increasingly faithful response of the Basin in more recent years.

Multiple processes have contributed to creation of the laminations in Santa Monica Basin. The principal factors appear to be (1) variations in porosity due to the relative abundance of organic filaments probably formed by *Beggiatoa* mats, and (2) compositional variations that reflect variations in carbonate/lithogenous ratios and in grain size. Both of these are expected to respond to ENSO events. The presence of near anoxic bottom waters has prevented bioturbation, permitting laminations to be preserved. Basin bottom waters became nearly anoxic about 350 years ago, at the onset of warming as the Little Ice Age waned. Expansion of the near anoxic area during the past century may have been augmented by 20th Century anthropogenic effects. The style of these non-annual laminations in Santa Monica Basin matches that of the annual laminations in the adjacent Santa Barbara Basin, and demonstrates the need for caution in interpreting all laminations as representing annual varves.

## Introduction

The classic "black shales" of the geologic record (e.g. Dunbar and Rogers, 1957; Calvert, 1986; Parrish, 1987) are now recognized to be the records of anoxic conditions in depositional sites spanning a spectrum of scales. Modern analogs of these anoxic depositional environments have been studied in many settings such as seasonal inner shelf anoxia (e.g. Rabalais et al., 1991), the Gulf of California (e.g. Calvert, 1966), the Black Sea (e.g. Ross and Degens, 1974), the Cariaco Basin (e.g. Richards and Vaccaro, 1956), and the upper slopes and outer shelves of the ocean's major upwelling regions such as the Chile–Peru margin (e.g. Reimers and Suess, 1983), and central and northern California (Gardner and Hemphill-Haley, 1986; Anderson et al., 1987, 1989, 1990; Dean et al., 1991). These are in areas that have been sites of strong seasonal upwelling, and/or restricted bottom water circulation (Ingle, 1981). In addition to the central California open slope,

[1]Present address: Amoco Production Company, 501 Westlake Park Blvd., P.O. Box 3092, Houston, TX 77253-3092, USA
[2]Author to whom all correspondence should be addressed

0025-3227/94/$07.00 
*SSDI* 0025-3227(93)E0131-O

the active margin basins of the California Borderland (Shepard and Emery, 1941) are silled basins which form settings for anoxic environments (Emery and Hulsemann, 1962; Malouta et al., 1981). Two of these, Santa Barbara and Santa Monica Basins, will be discussed in this paper.

In practice, terms from several disciplines including "anoxic", "hypoxic", as well as "anaerobic" in its original biological context, are generally used interchangeably (and probably incorrectly by geologists) to describe low-oxygen environments (see Tyson and Pearson, 1991). Rhoads and Morse (1971) developed a classification of oxygen-deficient environments that forms the basis for many workers in this field. They defined aerobic environments as those where oxygen content of the waters is greater than 50 $\mu M$ (1 ml/l). Content of 5–50 $\mu M$ (0.1–1.0 ml/l) defines the dysaerobic environment. In waters of less than 5 $\mu M$ (0.1 ml/l), conditions were defined to be anaerobic, and these waters contain insufficient oxygen to permit bioturbating organisms to survive. We will refer to basin waters with 0–5 $\mu M$ oxygen as near anoxic, the "anaerobic" environment of Rhoads and Morse (1971). The absence of bioturbation in anoxic and near-anoxic basins permits preservation of fine-scale depositional features that form laminations, and the existence of laminations is assumed to indicate the presence of anoxic or near-anoxic bottom waters.

The presence of low-oxygen basin-floor conditions in Santa Barbara Basin in the northern California Continental Borderland, and the preservation of primary nonbioturbated depositional laminae was first noted by Emery and Hulsemann (1962). Much work has been done in that basin to examine the mechanisms of formation of these deposits and their environment of deposition (e.g. Hulsemann and Emery, 1961; Sholkovitz and Gieskes, 1971; Drake et al., 1972; Sholkovitz, 1973; Soutar and Crill, 1977; Pisias, 1979; Thornton, 1981; Savrda et al., 1984; Reimers et al., 1990; Grant, 1991). Models proposed include (1) lamination attributed to alternations of diatom-rich layers deposited during high productivity seasons with detrital-rich layers deposited during wet seasons; (2) alternations in bacterial mat formation and degradation in which original mat zones exhibit bacterial filaments that support a more porous structure compared to non-mat hemipelagic deposition; (3) influence of nepheloid plume and muddy distal turbidite deposition during wet seasons, alternating with high biogenic deposits.

The laminated primary depositional facies in modern basin floor sediments in Santa Monica Basin (Fig. 1) were first described by Malouta et al. (1981). They assumed that the Santa Monica Basin laminae were annual couplets (varves) as had earlier been postulated for the Santa Barbara laminae (Soutar and Crill, 1977). This paper will describe new data that changes that assumption. In addition, whereas the Santa Barbara central basin floor has been in a predominantly near-anoxic condition for much of Holocene time (Pisias, 1979), the low-oxygen condition fostering preservation of the laminated facies in Santa

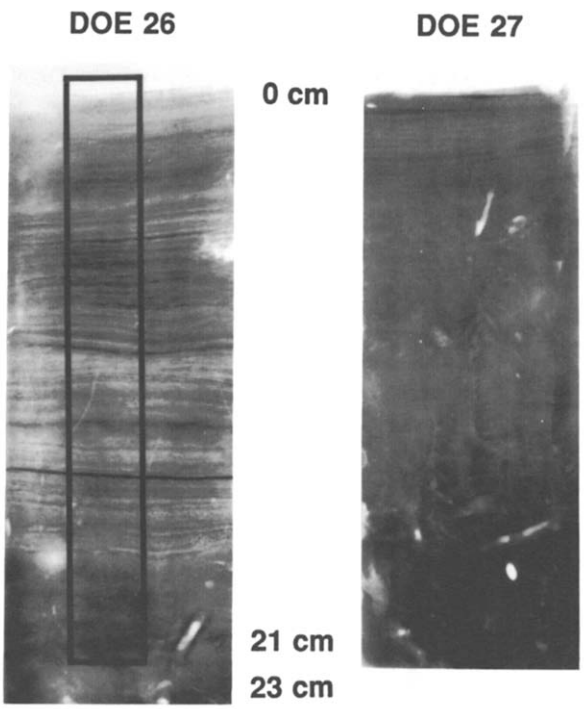


Fig. 1. Prints of radiograph films of the upper portions of box cores DOE 26 and 27 from the Santa Monica basin floor. DOE 26 is the longest nonbioturbated section (ca. 28 cm); DOE 27 is an example of cores on the fringe of the nonbioturbated anoxic zone (see Fig. 14). The area digitized of Core DOE 26 is outlined in black. Location is shown in Fig. 7. By convention, light laminations seen in this figure are classified as light in the text.

Monica Basin has been present only during the past four centuries or less (Huh et al., 1990; Christensen, 1991). This paper will summarize additional data showing the pattern of expansion of near anoxic bottom waters.

## The study locales

The California Continental Borderland (Shepard and Emery, 1941; Nardin, 1981; Teng, 1985; Gorsline and Teng, 1989; Lee, 1992) is a checkerboard morphology of deep basins classified on the basis of distance from mainland sediment sources into inner, central and outer basins (Gorsline and Emery, 1959; Emery, 1960; Fig. 2). Within this broad sequence of marginal basins and intervening banks and ridges, basin floor depths increase seaward and southward from 600 m to over 3000 m (Emery, 1960). Santa Monica Basin, the primary focus of this discussion, is an inner basin with a maximum basin floor depth of 910 m. Santa Barbara Basin is also an inner basin with a maximum depth of 600 m.

Within each basin, the sill depth is a major influence controlling the characteristics of the sub-sill basin waters (Emery, 1954; Doyle and Gorsline, 1977). Santa Barbara Basin's deepest sill at about 450 m provides a barrier to communication with the Pacific Ocean to the west, while the deepest sill to Santa Monica Basin is at 740 m, provides a barrier to exchange with San Pedro Basin to the south. North Pacific Intermediate Water (Emery, 1960; Reid, 1965; Hickey, 1979) is the source for water passing over the deep sills and gaps in the Patton Escarpment. The core of this water mass, centered around 500 m, has a strongly developed oxygen minimum with typical oxygen contents of $<20$ $\mu M$ (0.5 ml/l) (Reid, 1965). At intervals of one to several years, basins experience episodes of partial or nearly complete flushing, during which bottom water oxygen and nutrient concentrations will approach that of the source waters. These episodes are followed by a decline of bottom water oxygen over several months to a lower, quasi-steady state concentration that is maintained by a balance between downward diffusion and consumption. The drawdown time of bottom water oxygen in Santa Barbara Basin is of the order of 2–3 months (Sholkovitz and Geiskes, 1971; Reimers et al., 1990), and is similar to the drawdown of oxygen seen in data from Santa Monica Basin following the much less frequent intrusions

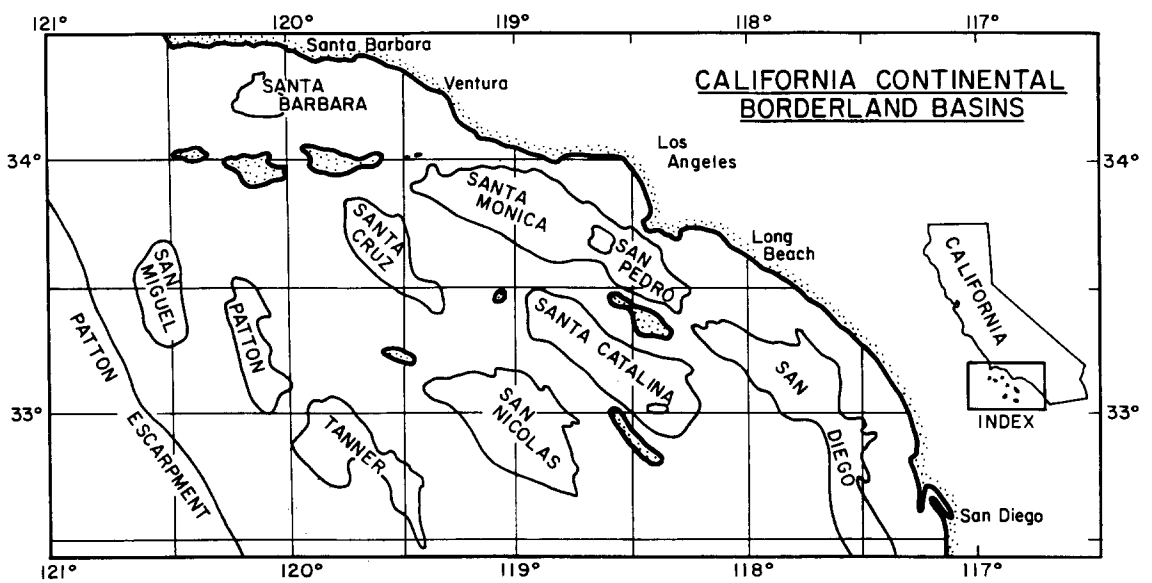


Fig. 2. Schematic map of the basins of the northern California Borderland showing the general outline of the closure of each basin. Maximum basin floor depth in Santa Barbara Basin is 600 m; maximum depth in Santa Monica Basin is 910 m; maximum depth in San Pedro Basin is 904 m.

that flush that basin's bottom waters (Hickey, 1991, 1992). Similar flushing characteristics have been described by Berelson (1991) in San Nicolas and in adjacent San Pedro Basin. Typical oxygen contents between times of bottom water intrusion in the lower 20–30 m of the water column are 3–7 $\mu M$ (0.07–0.15 ml/l) in Santa Monica Basin and 0–2 $\mu M$ (0–0.05 ml/l) in Santa Barbara Basin (e.g., CalCOFI, 1989, 1990, 1991).

Below 830 m water depth, the Santa Monica Basin floor is a near-horizontal depositional surface (surface gradients of 1–2′ of arc). The principal features are wide (3–4 km), low-relief (less than 5 m) levee–channel systems (Schwalbach and Gorsline, 1990; Gorsline, 1992; Schwalbach, Gorsline and Edwards, in review) (Fig. 3). These extend from the lower edge of Hueneme–Mugu Submarine Fan into the central basin floor, and influence the properties of the basin floor sediments since they are the principal conduits for turbidity currents and nepheloid plumes from the mainland slope, and from the basin floor distributaries. The Hueneme–Mugu Submarine Fan covers the northern third of the basin floor. Huh et al. (1990) showed that accumulation rates are relatively uniform across the basin floor, and that sediment trap fluxes near the basin center show only modest (ca. 20%) increases between 500 m and 850 m depth and are in good agreement with accumulation rates. These observations and the general absence of distinct turbidites (Reynolds, 1988) suggest most sediments reaching most of the central basin floor are hemipelagic and settle from the over-lying water column.

Santa Barbara Basin floor is a smooth plain that slopes gradually from the western sill at 450 m to a maximum depth of just over 600 m in a lateral distance of 35 km. From basin center to the eastern sill (a distance of 65 km), depth changes from just over 600 m to 250 m. Thornton (1981) shows that low-relief, low-angle slides are present in the lower slopes and basin plain. At the western end, the Conception Fan (Kraemer, 1986) has built a broad cone with a radius of about 25 km. This

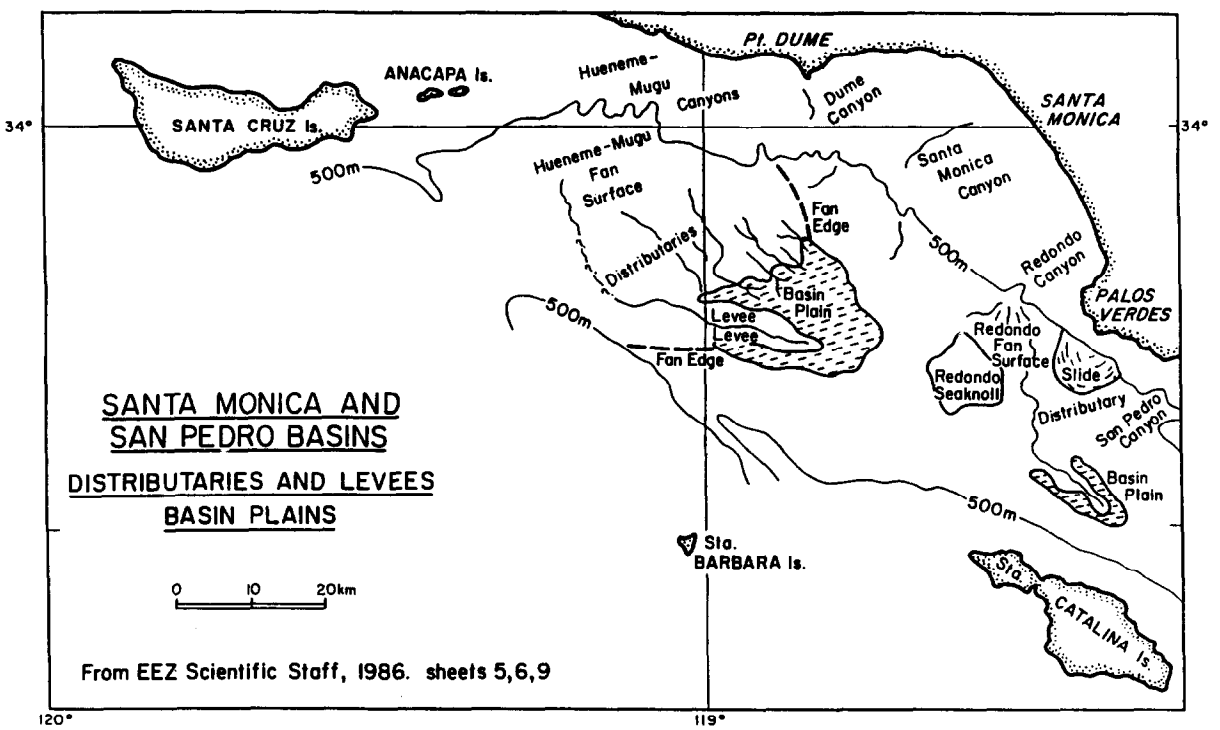


Fig. 3. Schematic geomorphic map of the basin floors of Santa Monica and San Pedro Basins showing the location of the basin plains, levee–channel systems extending into the basin plains from the fan margins. These are the contemporary active conduits for near-bottom and bottom suspension flows.

was active during low pre-Flandrian sea level. Nepheloid plumes move into the basin from east and west and from the mainland slopes (Thornton, 1981); turbidity currents are generated by mainland slope failures at intervals of a few hundred years. Basin floor sediments are hemipelagic muds whose general characteristics are shown in Table 1.

Savrda et al. (1984) noted the general absence of macrofauna and burrows in basin floor environments of Santa Barbara, Santa Monica and San Pedro Basins (from north to south) based on study of bottom photographs of those floors. Much earlier, Hartmann and Barnhard (1958) in a benthic biological survey of the Borderland basins noted the sparse benthic faunas in these same basins, and noted a few specimens of chemosymbiotic molluscs as being present. These observations confirm the absence of macrofauna. The areas of nonbioturbated basin-floor sediments give an integrated view of the areas of anoxic bottom water. In Santa Barbara Basin this zone includes approximately 400 $km^2$ of the deep central basin floor. In Santa Monica Basin, the area lacking bioturbation is 3 fold greater, over 1200 $km^2$. Where low oxygen prohibits burrowers, the primary laminated depositional structures of the hemipelagic muds are preserved (Fig. 1).

## Methods

### *Densitometer analysis of X-radiography*

Selected X-radiograph negatives of 7 central Santa Monica Basin cores were scanned using a Perkin-Elmer PDS Flatbed Densitometer, courtesy of the Jet Propulsion Laboratory's image processing facilities. The scans were made using a pixel size of 50 μm with vertical and horizontal positioning precision of about 1 μm. The densitometer was adjusted for each X-radiograph to enhance the optical density modulation in the laminated section of each box core. The most transparent area of a given radiograph negative was assigned a relative optical density value of 0 and the densest (darkest) area was assigned a relative optical density value of 255. A 2.5 cm wide vertical strip was digitized through the laminated section of each X-radiograph, resulting in 500 vertical profiles down each negative.

The selected pixel size represents about 5% of annual hemipelagic sedimentation laminae thickness. It is also equal to a coarse silt particle diameter. Smaller pixel size increases noise in the records. This pixel size is in the range used for scanning medical X-rays of comparable resolution. X-radiograph digitization was performed by Joseph Fulton of NASA's Jet Propulsion Laboratory, and the use of the facility was kindly provided by Dr. Ray Bambery. The digitized X-radiographs were recorded on magnetic tape and processed using software provided by Dr. Ray Bambery and computer programs written at the Department of Geological Sciences at USC. Details of the processing of the raw densitometer data are given by Christensen (1991).

The typical raw data on any vertical pass down each radiograph show a gradient of optical density in the top few centimeters of the radiograph that corresponds to the surficial compaction gradient in the accumulating sediments. This trend was removed from each of the digitized X-radiographs, and the data were corrected to the uniform mean-optical-density characteristic of the deeper compacted sediments. In modern basin floor sediments,

TABLE 1

Sediment characteristics for Santa Monica and Santa Barbara Basin floors. Mean value of each parameter and standard deviations about each mean are tabulated for all parameters. In Santa Barbara Basin, data are for the area deeper than 500 m. For Santa Monica Basin, data are for the area deeper than 800 m

| Basin | Mean diam. ($\phi$) | Std. dev. | Skewness | Kurtosis | $CaCO_3$ (wt.%) | TOC (wt.%) | Silt (wt.%) | Clay (wt.%) |
|---|---|---|---|---|---|---|---|---|
| Santa Monica | 7.3±0.9 | 2.0±0.2 | 0.1±0.4 | 2.0±0.7 | 7.2±3.6 | 3.4±1.6 | 56±11 | 39±11 |
| Santa Barbara | 7.3±0.7 | 2.0±0.1 | 0.2±0.4 | 2.1±0.5 | 6.9±2.4 | 3.1±1.2 | 59±9 | 37±12 |

surface bulk density is of the order of 1.1–1.2 gm/cm$^3$, increasing to about 1.3–1.5 gm/cm$^3$ at a depth of 10–15 cm (Reynolds, 1988). To reduce signal noise, vertical scan paths were filtered using a running average of four adjacent pixels.

Selected vertical scans at 0.5 cm width intervals (10 scans) were adjusted to flatten laminations and stacked to produce a representative stacked profile of relative optical density for each radiograph (Figs. 4 and 5). In addition, the records from each core were corrected for missing core top material using bulk density measurements, and by matching strong laminae contrasts. The box coring method is generally effective in capturing surface material, but some very low density material can be washed or "blown out" during the coring process. $^{210}$Pb data also were used to confirm core loss.

The processed, digitized X-radiographs produce a quantitative representation of the light–dark couplets in each core. These laminae count data can then be compared to time to define the actual frequency and duration of each couplet. The convention that will be used in this study is that seen in prints of X-radiographs: light laminations have lower density and permit more X-ray penetration than dark laminations. Thus, in the densitometer records shown, maxima define light laminae and minima define dark laminae.

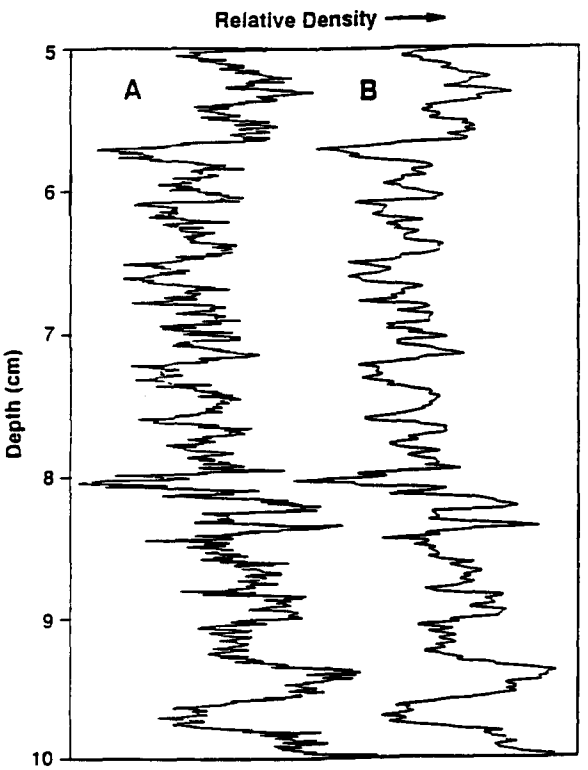


Fig. 4. Example of smoothing of individual vertical scans by using running average of four in sequence. Data are from DOE 26 (see Fig. 1 for radiograph). A is raw data and B is smoothed data. Plot is for line 250 of relative density versus depth in core. This line is mid-core (width of 500 lines of 50 μm pixel widths). See location in Fig. 7.

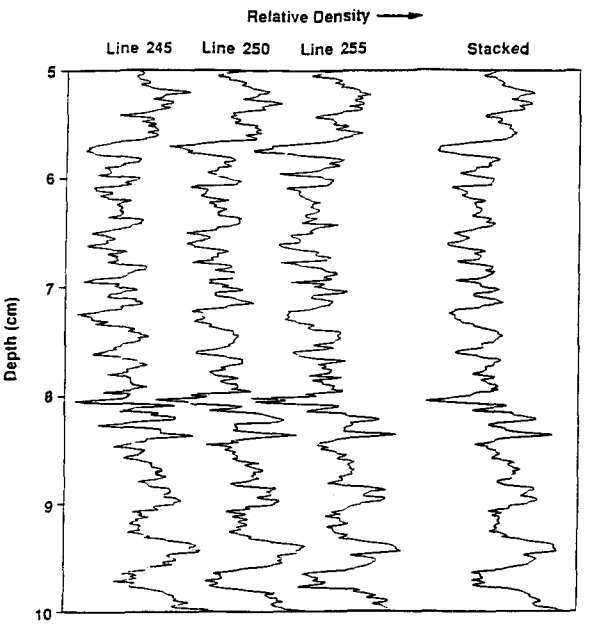


Fig. 5. Graph illustrating effect of stacking several smoothed vertical scans of digitized data to obtain a single stacked profile representative of the radiograph. Data are from DOE 26. These are three equally spaced central lines (0–500 line width). Location is shown in Fig. 7.

### *$^{210}$Pb and porosity*

Box cores were collected and sectioned after retrieval into intervals 1–2 cm in thickness, with 8 to 10 different depth intervals in each box-core. No samples were taken below 16 cm since $^{210}$Pb was assumed to be in equilibrium with $^{226}$Ra at depth. Huh et al. (1987) observed decreases in $^{210}$Pb activities in the top 1 cm of sediment in box-cores from Santa Monica Basin and suggest this decreased activity is associated with changing redox conditions below the sediment–water interface. The top sediment interval of the DOE cores

used in this study was not sampled to avoid any discontinuities in $^{210}$Pb activities. The $^{210}$Pb activity of each sample was found by measuring the activity of $^{210}$Pb's grand-daughter $^{210}$Po and assuming secular equilibrium between the two isotopes. This assumption should be valid since the top centimeter of sediment was not sampled and more than twenty $^{210}$Po half-lives had elapsed between deposition of the remaining box-core material and analysis of sediment intervals.

$^{210}$Po was measured as outlined by Fuller (1982). Briefly, the samples were dried at 110°C for 24 hours and crushed into a fine powder. Approximately 0.2–1.2 g of sample was totally dissolved by successive treatments with hydrochloric, nitric and perchloric, and hydrofluoric acids. Approximately 15 dpm of $^{208}$Po spike was added to each sample during the dissolution. This spike was calibrated against a $^{210}$Pb standard obtained from the United States Environmental Protection Agency. After the dissolution steps, the samples were dried, the residues were washed several times with 8.0 *N* HCl to ensure removal of all $HNO_3$ and redissolved in 1.0 *N* HCl. Ascorbic acid was added to complex iron, and Polonium was plated onto 1.2 cm silver disks at 90°C.

Alpha spectroscopy was used to measure $^{210}$Po/$^{208}$Po. A minimum of 1200 counts was obtained for both $^{210}$Po and $^{208}$Po peaks so that $1\sigma$ counting errors would be less than 3%. Both peaks were corrected for counter background and $^{208}$Po peaks were corrected for tail effects from $^{210}$Po peaks (Christensen, 1991).

Composites of the solutions remaining after plating were placed in sealed glass bottles for $^{226}$Ra determinations by using techniques of Mathieu et al. (1988) to measure $^{222}$Rn ingrowth. Composites were made from upper (typically $<8$ cm) and lower (typically $>8$ cm) samples. Replicate analyses were run for all sample bottles to reduce measurement errors. All sediment dry weights have been corrected for salt content.

For most cores, little difference was observed between upper and lower $^{226}$Ra composites and the $^{210}$Po measured below 12 cm core depth. Exceptions were composites with turbidite horizons or a few composites that contained a small amount of black residue, apparently from an incomplete digestion. Based on the $^{226}$Ra composites and the deep $^{210}$Po, supported values of $^{210}$Pb were estimated for each core, ranging from 7.5 to 8.5 dpm/g. This value was subtracted from the measurements of $^{210}$Po to obtain excess $^{210}$Pb.

Porosities were not measured on the samples in this study because of pore water loss during sectioning and storage. Salt corrections and integrated density calculations were done using porosity values from Huh et al. (1987) and C.A. Huh (unpubl. data). Porosity profiles from four box-cores located in the deep ($>870$ m), central portion of Santa Monica Basin were used to estimate porosities in the box-cores sampled in this study. Porosity profiles are plotted in Fig. 6 and the locations of cores used are shown in Fig. 7. Porosity profiles are relatively uniform across the deep basin and are characterized by a large decrease in porosity in the top few centimeters of each core from as much as 96% at the surface to roughly 87% at a depth of 5 cm. Below 5 cm, porosity decreases more slowly and has an average value of about 86% between 5 to 25 cm core depth (also see microfabric observations by Reynolds, 1988). Porosity values for the box-cores sampled

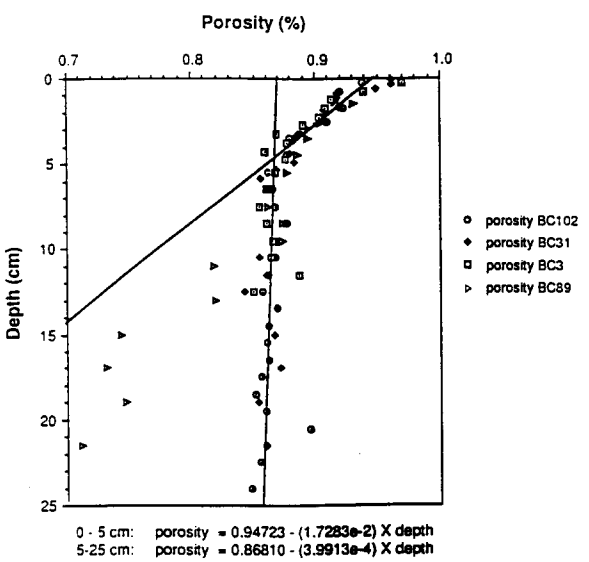


Fig. 6. Porosity data for a selection of box cores from Huh and others (1987). Lines are linear regressions of data from 0 to 5 cm and 5 to 25 cm. Core BC89, on the western margin of the deep basin, contains a turbidite that causes the decrease below 10 cm. These deeper intervals were excluded from the fit.

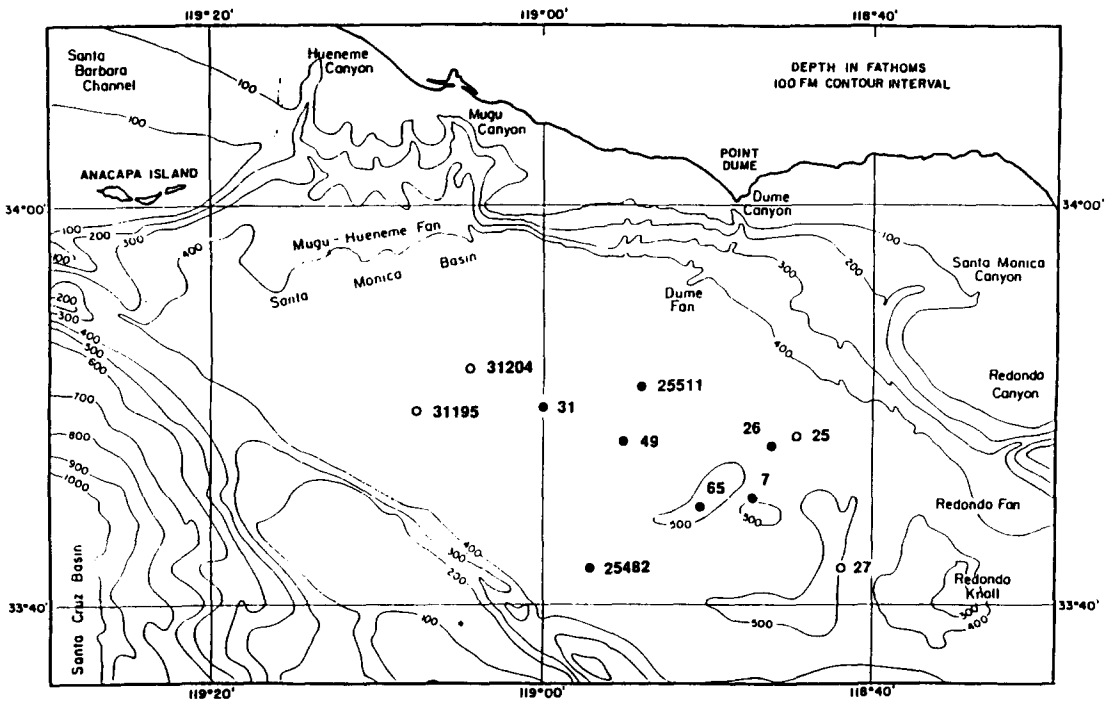


Fig. 7. Locations of box cores sampled for this study. Five digit numbers are AHF cores and two digit numbers are DOE cores. Filled circles represent cores whose radiograph negatives were digitized.

in this study were estimated by fitting lines to these two trends using linear least squares. The porosity profile of core CaBS I BC89 was taken in the western portion of Santa Monica Basin, and the porosity discontinuity in this core is associated with a turbidite. Therefore, porosity data below 10 cm in core CaBS I BC89 were ignored when trends were fitted to the data of Fig. 6.

## Results

### *Chronology from $^{210}Pb$*

Two assumptions must be made before the $^{210}Pb$ method can be applied. First, one must assume that the supply of $^{210}Pb$ to the sediment in a given location is constant over time, and second, one must assume little or no mixing of sediment has occurred. While the seasonal and interannual changes in sedimentation rates and particulate composition may affect $^{210}Pb$ activities in the water column, $^{210}Pb$ flux to the sediments is relatively constant over the multi-year periods represented in sample intervals (Koide et al., 1972, 1973; Huh et al., 1987, 1990). The laminated nature of the sediments in this study suggest that bioturbation is minimal and the second assumption appears to be valid. However, excess $^{234}Th$ profiles show that some mixing occurs in the top 1 cm of sediment cores recovered from Santa Monica Basin. This mixing may occur during recovery and sectioning of box-cores (Huh et al., 1987). One additional assumption made here was that supported $^{210}Pb$ is constant with depth, based on the $^{226}Ra$ measurements.

Accumulation rates were derived by fitting excess $^{210}Pb$ versus cumulative density in each core. Cumulative density was calculated as the integral of dry density versus depth, using the regression to porosity profiles (Fig. 6), and a solid phase density of 2.5 g/cm$^3$. The data were fit with an exponential function to derive sedimentation rates, using a least squares technique described by Wolberg (1967). When this method of exponential least squares is applied to $^{210}Pb$ profiles, individual samples are weighted by their respective uncertain-

ties, and low activity samples, with relatively high uncertainties, are not weighted as heavily as high activity samples. The $^{210}$Pb sedimentation rates calculated using the exponential least squares method are theoretically better than rates calculated using traditional methods. Uncertainties (Table 2) represent one standard deviation of the derived accumulation rates.

Total and excess $^{210}$Pb profiles are shown in Fig. 8a–k, along with the fits used to derive sedimentation rates. Excess $^{210}$Pb activities were calculated by subtracting the supported $^{210}$Pb activities from the total $^{210}$Pb activities. Results are not very sensitive to the choice of supported $^{210}$Pb (Table 2). Sedimentation rates for cores AHF31195 and AHF31204 could not be calculated because of their anomalous $^{210}$Pb profiles. These cores are located on the distal portion of the Hueneme–Mugu Submarine Fan, and the large variations observed in $^{210}$Pb activity with depth in these cores are most likely due to the presence of numerous turbidites. Box cores AHF24582 and DOE31 contained marked sediment discontinuities at a depth of roughly 10 cm. Although discontinuities were not found in all cores, excess $^{210}$Pb activities for samples below 10 cm were not used to calculate sedimentation rates for consistency. Excess $^{210}$Pb activities are relatively low below this depth, and lithologic variability can add very large uncertainties to these data points.

Sedimentation rates range from 13.3 to 20.8 mg/cm$^2$/yr, with a standard deviation of 2.8 mg/cm$^2$/yr. The average sedimentation rate of the nine box cores used in this study is $16.0 \pm 0.4$ mg/cm$^2$/yr. This average was calculated by weighting each sedimentation rate by its associated uncertainty, and the uncertainty reported is the standard error of the mean. Assuming an average porosity of 86% at depth and a sediment density of 2.5 g/cm$^3$, sediment accumulation rates range from 0.38 to 0.59 mm/yr, with an average of 0.46 mm/yr (46 cm per 1000 yr).

The $^{210}$Pb sedimentation rates reported here for deep Santa Monica Basin are lower than those reported by early workers, e.g. 24 mg/cm$^2$/yr by Bruland et al. (1974) and 21 to 28 mg/cm$^2$/yr by Malouta et al. (1981), but are in good agreement with more recent work, e.g. 19 mg/cm$^2$/yr by Bruland et al. (1981) and 14.1–18.8 mg/cm$^2$/yr by Huh et al. (1990). The principal cause of higher sedimentation rates reported in the two early studies is due to their use of erroneously high values of bulk density to convert depth-based sedimentation rates (centimeters per year) into mass sedimentation rates. Additional differences are due to differences in the methods Bruland et al.

TABLE 2

Calculated $^{210}$Pb sedimentation rates and sensitivity to changes in supported $^{210}$Pb. The weighted average has been weighted by the inverse of the square of the standard deviation for each profile

| Box core no. | Supported $^{210}$Pb (dpm/g) | Sedimentation rate using supported $^{210}$Pb (mg/cm$^2$/yr) ($A$) | Sedimentation rate with supported $^{210}$Pb = 8.0 dpm/g (mg/cm$^2$/yr) ($B$) | % Difference $(B-A)\times 100/A$ |
|---|---|---|---|---|
| AHF25482 | 8.5 | $17.8 \pm 1.3$ | $19.1 \pm 1.4$ | +7.3 |
| AHF25511 | 7.5 | $15.1 \pm 1.1$ | $14.6 \pm 1.1$ | −3.3 |
| DOE 07 | 8.0 | $14.8 \pm 1.9$ | $14.8 \pm 1.9$ | – |
| DOE 25 | 7.0 | $20.8 \pm 4.9$ | $17.8 \pm 3.8$ | −14.4 |
| DOE 26 | 8.0 | $17.7 \pm 0.8$ | $17.7 \pm 0.8$ | – |
| DOE 27 | 7.5 | $20.1 \pm 2.3$ | $19.2 \pm 2.1$ | −4.5 |
| DOE 31 | 8.0 | $13.3 \pm 0.9$ | $13.3 \pm 0.9$ | – |
| DOE 49 | 8.5 | $19.1 \pm 0.9$ | $19.6 \pm 0.9$ | +2.6 |
| DOE 65 | 8.5 | $13.6 \pm 0.8$ | $14.2 \pm 1.1$ | +4.4 |
| Simple ave. ±1 se | | $16.9 \pm 0.9$ | $16.7 \pm 0.8$ | |
| Weighted ave. ±1 se | | $16.0 \pm 0.4$ | $16.4 \pm 0.4$ | |

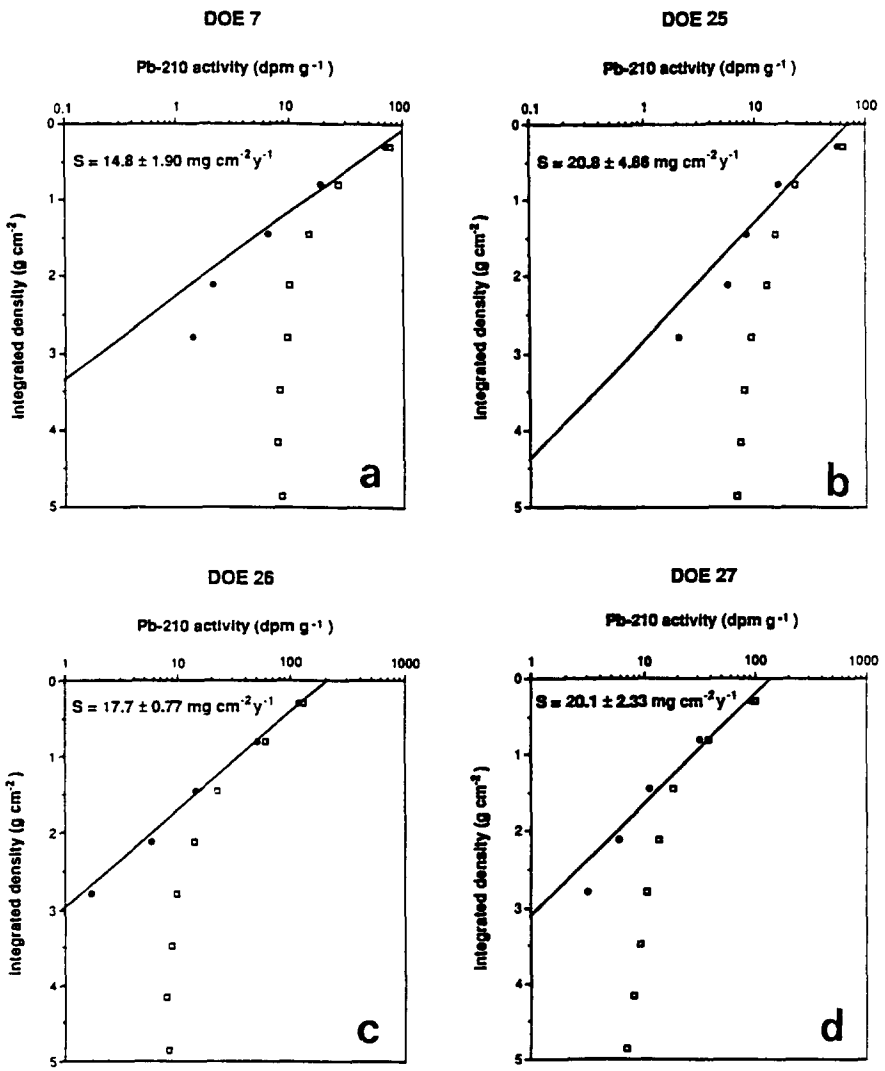


Fig. 8a–d.

(1974) and Malouta et al. (1981) used to measure $^{210}$Pb activities and calculate sedimentation rates. Sediment samples in both studies were not completely digested, resulting in under-estimation of supported $^{210}$Pb. In addition, sedimentation rates in these two studies were calculated by fitting profiles of excess $^{210}$Pb versus depth instead of integrated density (cumulative dry mass).

Huh et al. (1990) found accumulation rates on the eastern side of the basin were slightly higher than in the center. Our most central cores (DOE 7 and 65) do have lower accumulation rates than others, but the data set as a whole does not indicate any simple spatial pattern when grouped with that of Huh et al. (1990). Thus, we will use a uniform accumulation rate for all central basin cores.

*Lamination frequency*

Given a time scale from the $^{210}$Pb chronology, and the quantitative couplet record (light–dark cycles) from the digitized X-radiographs, the duration of the couplets can be calculated and the frequency distribution of these durations analyzed. For each core, the vertical reference of the stacked relative-density profile created from the corre-

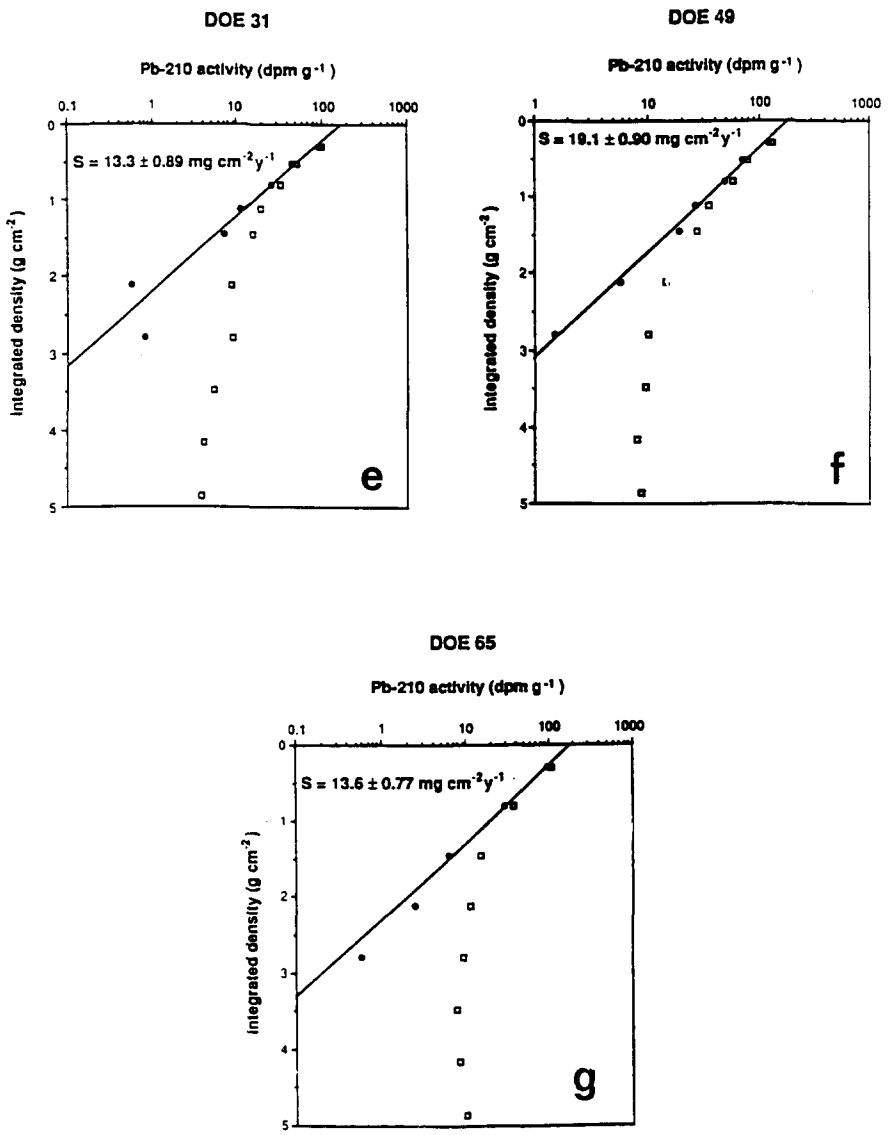


Fig. 8e–g.

sponding digitized X-radiograph was converted from depth to time by converting porosity into integrated density and then dividing integrated density by sedimentation rate. Figure 9 shows these records for seven cores distributed over the basin floor using the average accumulation rate of 16 mg/cm$^2$/yr. Although individual laminae are difficult to trace from core to core, two distinct spikes in relative density (marked with arrows in Fig. 9) occur at 170–180 yrs B.P. and at about 230 yrs B.P. Four records also show a spike at about 260–270 yrs B.P. The apparent synchroneity of these events supports the model of uniform basin floor hemipelagic deposition suggested by the $^{210}$Pb data.

The frequency distribution of laminae couplets in Santa Monica basin was analyzed by writing a computer algorithm to pick light and dark laminations. The algorithm uses changes in slope between adjacent data points in the stacked relative-density records to identify minima (dark laminations) and maxima (light laminations). A cutoff

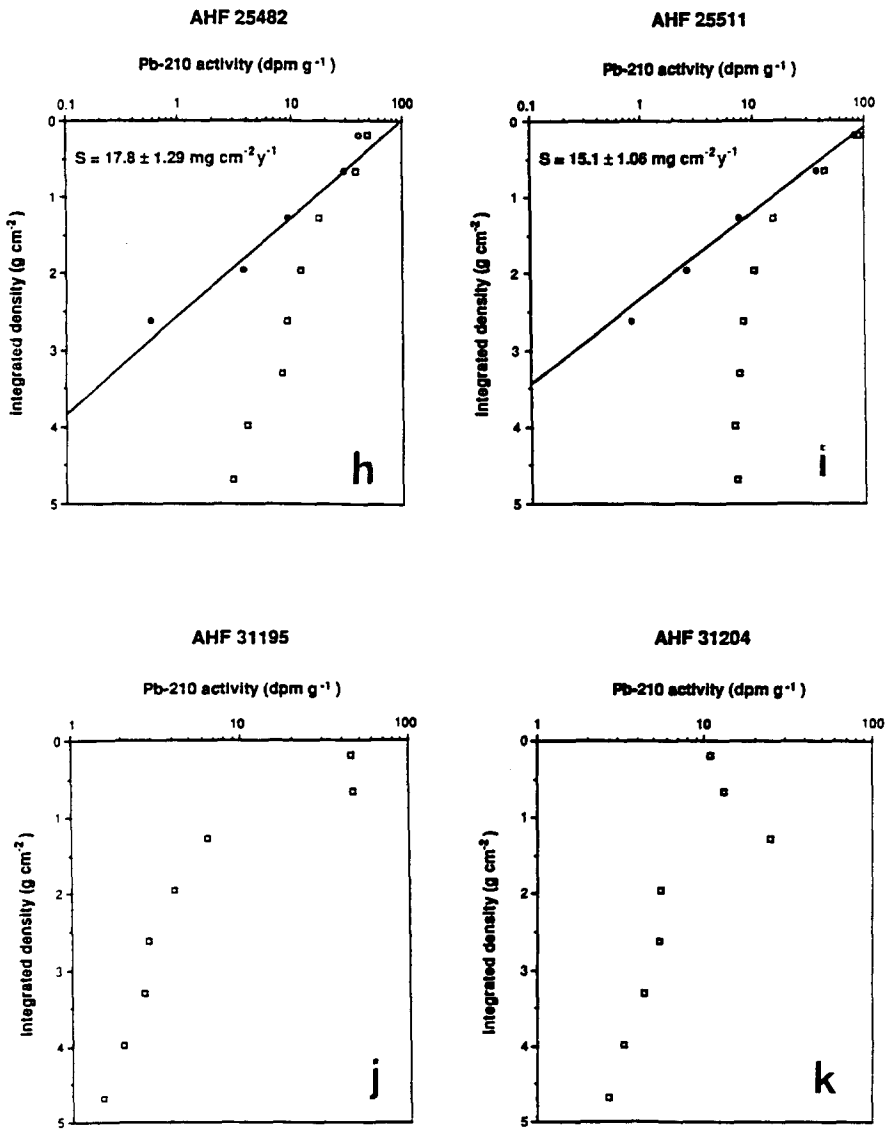


Fig. 8. $^{210}$Pb profiles (a–k). Open symbols ate total $^{210}$Pb and filled symbols are excess $^{210}$Pb. Lines show least square fits of exponential function to excess $^{210}$Pb using technique described by Wolberg (1967). Profiles (j) and (k) appear to be influenced by turbidites and were not fit.

value of 2 units of relative optical density, twice the uncertainty associated with digitization, was used to eliminate minor extrema. Laminations were also picked visually, using image processing software provided to USC by Dr. Ray Bambery of NASA's Jet Propulsion laboratory, in order to ensure that no significant signal was lost during processing of the digitized X-radiographs. The image processing software made it possible to zoom-in on small areas of the digitized X-radiographs and visually locate the positions of individual laminations. A comparison of laminations picked visually and laminations picked by the computer algorithm for core DOE 26 indicates that the results of both approaches are similar (Fig. 10).

In the first report of these laminated sediments (Malouta et al., 1981) it had been assumed that the laminae in Santa Monica Basin were annual couplets (varves) similar to those in Santa Barbara

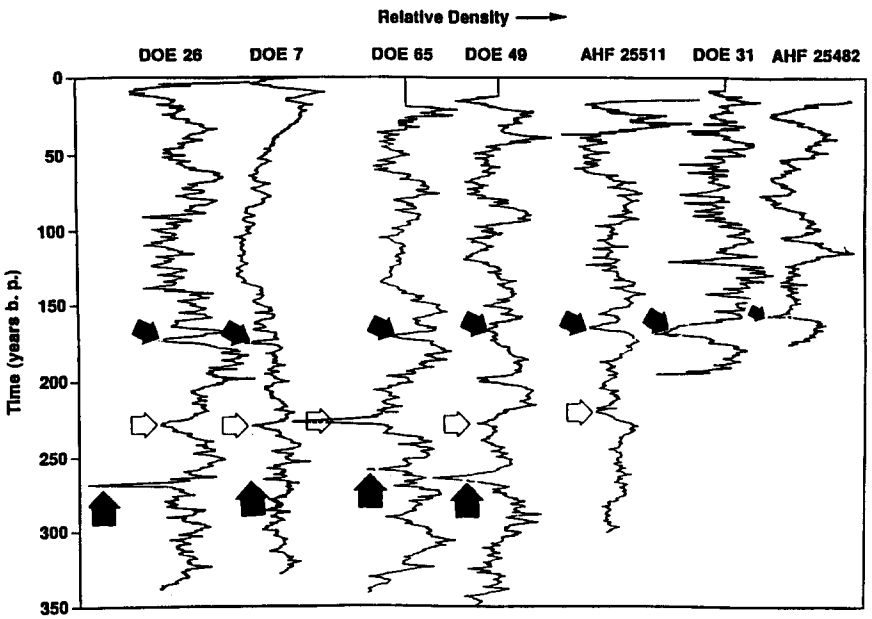


Fig. 9. Relative density versus time profiles of 7 cores (see Fig. 7 for locations). Sedimentation rates for all are assumed to be basin floor average of 16 mg/cm$^2$/yr. Arrows indicate correlated spikes of low relative density at 170–180 yrs B.P. (solid arrows), 230 years bp (open arrows), and 270 years B.P. (solid arrows).

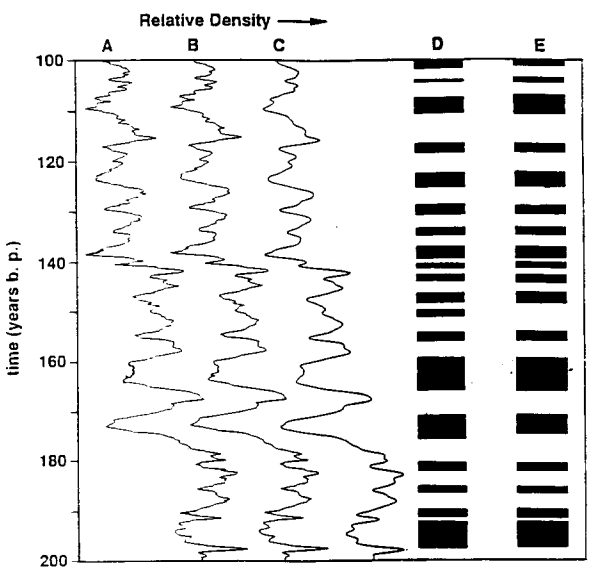


Fig. 10. Methods used to analyze lamination time series, illustrated by a section of DOE 26. (A) Stacked raw data; (B) Interpolation to obtain evenly spaced time series (0.2 year spacing); (C) Time series smoothed with 3 point running mean (0.6 year bandwidth); (D) Laminations chosen visually; (E) Laminations chosen by computer algorithm.

Basin. Figure 11 shows the histogram of durations of couplets in Santa Monica Basin sediments based on $^{210}$Pb dating. Over half of these couplets have a duration in the 3–7 year range, and only infrequently (less than 2%) is the duration annual. Durations can be as much as decadal at the far end of the spectrum. The median of this distribution is 6.0 years.

These frequencies closely match those of the El Niño-Southern Oscillation frequencies (Cane, 1983; Cane and Zebiak, 1985; Quinn et al., 1978, 1987). Quinn et al. (1978) tabulated historic occurrences of El Niño conditions to show that 50–52% of the events have frequencies of 3–6 years.

Histograms of lamination duration for one hundred year time intervals were also computed (Fig. 12). These show a slight (and marginally significant) shift toward a higher proportion of longer period events. Medians for each century are 5.2, 6.4, and 7.0 years, increasing with increasing age. Because this time period exceeds the range of the $^{210}$Pb dating, the slight shift can be interpreted in any of several ways: (1) sediment accumulation rates were higher in the past than at present, (2) ENSO forcing events were less frequent in the

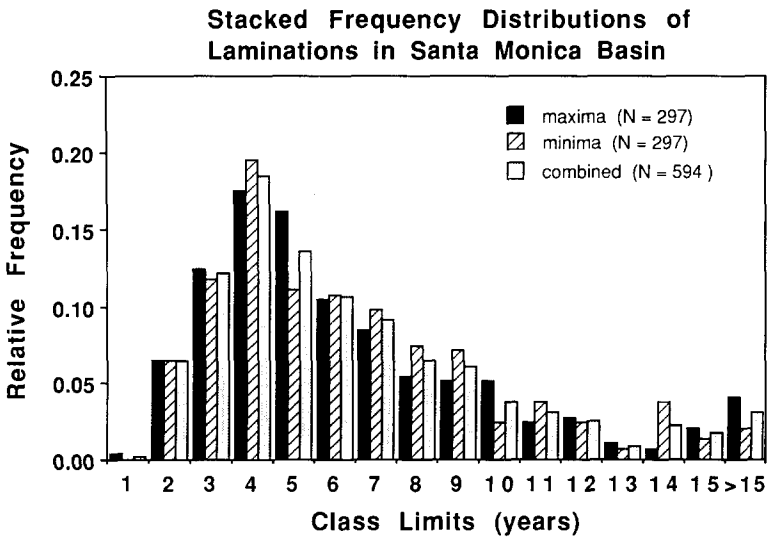


Fig. 11. Composite histogram of laminae durations in the 7 basin floor cores studied. Comparisons are made of laminae duration based on selection using radiograph density maxima (light laminae) separation, minima (dark laminae) separation, and combined dark–light couplets. The median duration is 6.0 years.

past, or (3) the Basin was less responsive in the past so that fewer weak and moderate events were recorded. It is likely that the first possibility has played some role, because the course of the Los Angeles River has alternated from discharging westward, into Santa Monica Bay north of the Palos Verdes Peninsula (Fig. 3), to discharging southward, into San Pedro channel east of this peninsula. For an unknown period prior to 1825, discharge was westward, but during the floods of that year the course shifted to the south (Poland et al., 1959). During the floods of 1862 and 1884, part of the flow discharged westward again, but since then, the flow has remained southward (Troxell et al., 1942). These changes may have reduced sediment input to Santa Monica Basin during the past 100–200 years.

*Distribution and causes of undisturbed primary laminations*

Using the uniform accumulation rate defined by the $^{210}$Pb method, radiographs of about 30 box cores were examined to establish the time of initiation of near anoxia at each core station, assuming that the presence of laminations is a proxy for near anoxia. Plotting these data (Fig. 13) shows that the near anoxia began in the deep central basin floor about 350 yrs B.P. and then progressively spread over the basin floor. A similar conclusion was reached by Huh et al. (1990) based on a more limited data base. Possible causes of the spread of near anoxic waters include increases in the flux of reactive organic matter to the sea floor, a reduction in bottom water mixing or exchange rates in response to a change in thermal structure, or a decrease in oxygen concentration in the North Pacific Intermediate Water. These possibilities cannot be distinguished at present. During the past century, increases in organic carbon supply from sewage discharges (Jackson et al., 1989), may have augmented natural events. The onset of near anoxia corresponds to the decline of the Little Ice Age in Europe (ca. 1450–1850), although the significance of this timing is not clear.

It is tempting to try to correlate individual laminae with distinct ENSO events. Although there is a general trend in duration that matches the variations in the Southern California rainfall record, it is difficult to make a unique correlation using the observations described here (Christensen, 1991).

Based on studies of others, we infer two principal mechanisms as the primary causes for laminae

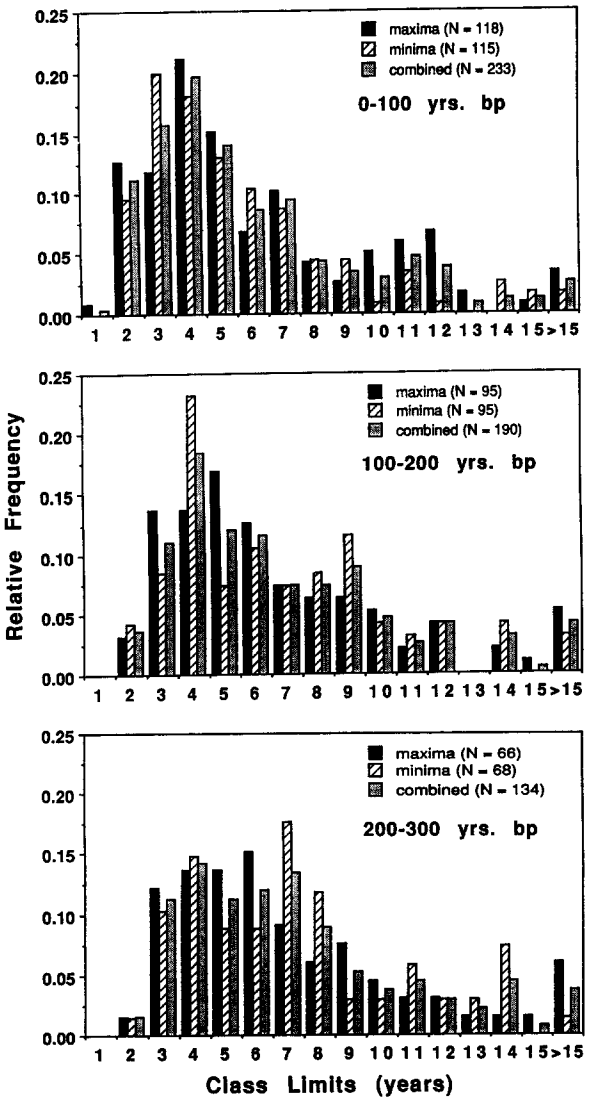


Fig. 12. Composite histogram of laminae duration in the 7 basin floor cores studied, shown for one hundred year intervals. Note that the number of laminations refers to the total for all cores. The medians for each panel (top to bottom) are 5.2, 6.4, and 7.0 years.

formation in Santa Monica Basin. Reynolds (1988) has examined the microfabric of Santa Monica Basin floor sediments. She observed laminae of mm scale in freshly cut cores, but these disappeared rapidly after exposure to air. Laminae were clearly apparent in X-radiography, but they were more difficult to identify with electron microscopy. Using the latter technique she noted ubiquitous bio-aggregates and that early diagenetic compaction reduces pore space and compresses packing of clay domains around silt grains within the top 10–15 cm. A few laminae showed graded bedding and could be attributed to turbidites. Most laminae were subtle and appeared to reflect organic or textural "stringers" that influence packing. Thus, the laminae seen in X-radiography are probably attributable to fine-scale porosity variations with some minor compositional variations. The differences in relative optical density that define a lamination are typically 1–10%, and the variations in particle packing (or X-ray density) must be less than this because of the definition of the scale zero. The source of the "organic stringers" are very likely bacterial filaments of *Beggiatoa* mats that have been observed on the surface of these sediments (by DSG) and those of Santa Barbara Basin (Soutar and Crill, 1977; Reimers et al., 1990). Grant (1991) noted that where these filaments are present in Santa Barbara Basin sediments (recording past mats) they tend to hold the microfabric in a more open packing (lower density). "Textural stringers" appear to reflect a slight grain size variation and are sometimes characterized by foram-rich layers (Reynolds, 1988). This corroborates a few SEM–EDAX measurements made by Malouta (1978) that showed some "light" layers may contain approximately twice as much carbonate as their darker counterparts. Consequently, laminations in Santa Monica Basin may reflect an alternating appearance of *Beggiatoa* mats or episodic large pulses of lithogenous material.

Both of these phenomena should respond to ENSO events. Soutar and Crill (1977) and Reimers et al. (1990) have shown that *Beggiatoa* mats in Santa Barbara basin grow and die as the basin bottom waters undergo an annual oscillation in oxygen concentration due to bottom water renewal each spring. In deeper basins of the Borderland, flushing events occur less frequently and are a response to regional changes in the density field during El Niño years (Berelson, 1991; Hickey, 1991). For example, Berelson (1991) has shown that adjacent San Pedro Basin has multi-year variations in bottom water oxygen concentration, responding to ENSO perturbation, and one of us (D.E. Hammond, unpubl. data) has observed at

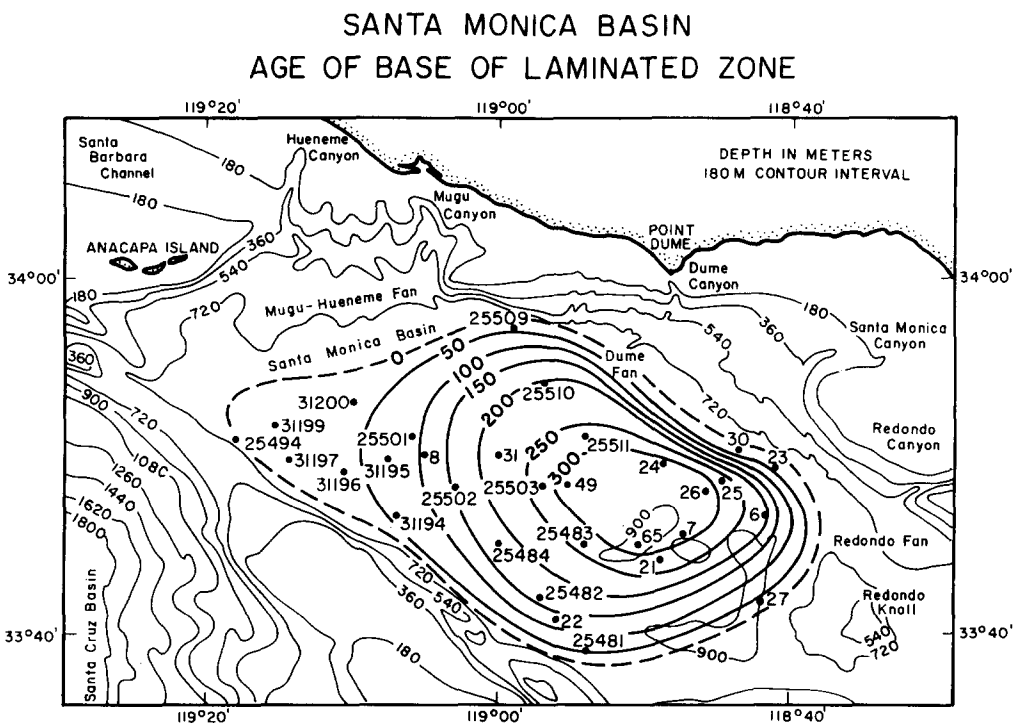


Fig. 13. Map of isochrons of time of initiation of near anoxia in basin bottom waters. Time is based on $^{210}Pb$ dating of sediments deposited during the past century, extrapolated to the base of laminated zone in each box core. Core locations used to control contours are shown. Undated cores were also used to add detail (locations not shown).

least one episode of oxygen-rich bottom water entering Santa Monica Basin during the spring of 1988, following an ENSO winter. Input of lithogenous sediment is dependent on rainfall in southern California, and consequently on ENSO events. Storage of sediment on shelves modulates the pattern (Drake et al., 1972) and may filter the higher frequency annual cycle into an interannual pattern. Periods with less lithogenous input could lead to the carbonate-rich layers or grain size variations observed with electron microscopy. It is interesting to note that light laminae (lower X-ray opacity) are an average 20–30% thicker than dark laminae (Christensen, 1991).

Examination of X-radiographs of approximately 50 box cores in Santa Monica Basin has defined the geographic limits of the nonbioturbated fine basin hemipelagic sediment of the basin floor (Fig. 14). The radiographs also show that the maximum thickness of the laminated facies in the central zone (deposited from about 350 yrs B.P.) is about 28 cm. The present edge of the nonbioturbated field is at variable water depth, as shown in Fig. 14. This non-level surface reflects a dynamic influence, since it is obvious that the anoxic area is not a simple pond in the deepest basin floor outlined by a single isobath. Relief of the outline is about 70–80 m. This may reflect the environmental boundaries of the bioturbating fauna which are controlled by bottom water oxygen content and the source of bottom water renewals.

In contrast, Santa Barbara Basin near anoxic floor conditions have been operative for much of Holocene time, but the balance between oxygen supply and demand is much affected by the more rapid circulation, shallower water depth, higher sedimentation rates, and annual recharge in that basin (Soutar and Crill, 1977; Reimers et al., 1990). This produces a much less continuous record in which major flood-generated uniform gray silt layers, thin distal turbidites and bioturbated layers interrupt the nonbioturbated sequence on a centi-

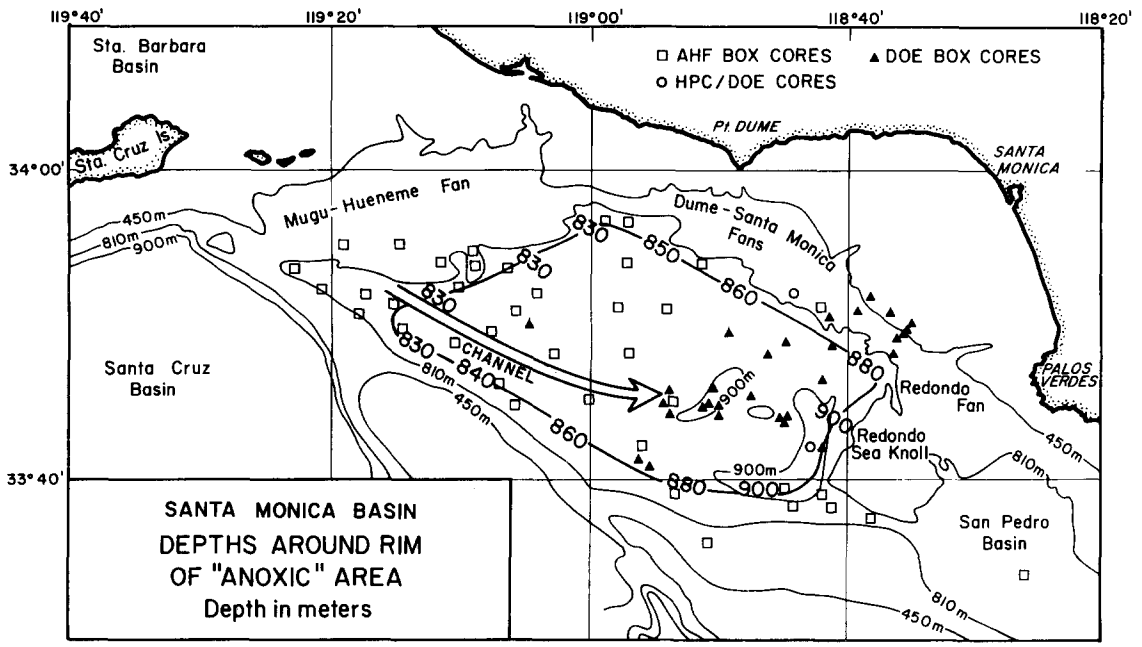


Fig. 14. Map of the depth of the edge of the present area lacking bioturbation. Note that the surface is tilted to the southwest and reflects the influence of bottom water motion (basal gyre) on extent of oxygen-deficient zone. Maximum relief is about 70–80 m along a NW–SE axis through the lens.

meter scale. Santa Monica Basin's laminated lens is strikingly continuous and shows no interruptions except for an occasional turbidite.

## Conclusions

The accumulation rate of hemipelagic sediments on the deep basin floor has been relatively uniform during the past century at $16.0 \pm 0.4$ mg/cm$^2$/yr, based on $^{210}$Pb analyses. This rate is in good agreement with previous work (Bruland et al., 1981; Huh et al., 1990).

The combination of densitometry to quantitatively define the light–dark alternations seen in radiographs of basin floor cores, and rates of accumulation determined by $^{210}$Pb analyses, show that the laminae couplets in nonbioturbated Santa Monica Basin hemipelagic sediments are not varves. Rather, they have durations that range from annual to decadal and a mean duration of 3–7 years, a period comparable to the El Niño-Southern Oscillation recurrence interval. The record shows a slight increase in couplet duration with increasing age, a trend that may reflect higher sedimentation rates in the past, a decreasing frequency of forcing events in the past, or a less faithful response of the basin to the forcing function in the past.

The observations reported briefly here support laminae couplet formation models that are strongly related to bacterial mat formation and degradation (Soutar and Crill, 1977; Reimers et al., 1990; Grant, 1991) or major pulses of detrital sediment input, two phenomena that should respond to ENSO forcing. The style of these non-annual laminations in Santa Monica Basin is quite similar to that of the annual laminations in Santa Barbara Basin. From a stratigraphic point of view, these conclusions would argue for caution in interpreting laminae couplets in "black shales" as varves.

## Acknowledgments

Cooperative data and information from Dr. C.A. Huh (Oregon State University) and Drs. K. Wang and V. Noshkin (Lawrence Livermore National Laboratory) facilitated this study. Funding over the years has come from Ocean

Sciences Division, National Science Foundation and the Environmental Research Section, Department of Energy.

Drs. Mary Scranton, Clare Reimers, Gabe Filipelli, and Whitey Hagadorn provided critical reviews that materially improved the paper.

## References

Anderson, R.Y., Gardner, J.V. and Hemphill-Haley, E., 1987. Persistent late Pleistocene–Holocene upwelling and varves off the coast of California. Quat. Res., 28: 307–321.

Anderson, R.Y., Gardner, J.V. and Hemphill-Haley, E., 1989. Variability of the late Pleistocene–Holocene oxygen-minimum zone off northern California. In: D.H. Peterson (Editor), Aspects of Climatic Variability in the Pacific and Western Americas. (Geophysical Monograph, 55.) Am. Geophys. Union, pp. 75–84.

Anderson, R.Y., Linsley, B.K. and Gardner, J.V., 1990. Expression of seasonal and ENSO forcing in climatic variability at lower than ENSO frequencies: evidence from Pleistocene marine varves off California. Palaeogeogr., Palaeoclimatol., Palaeoecol., 78: 287–300.

Berelson, W.M., 1991. The flushing of two deep sea basins, Southern California Borderland. Limnol. Oceanogr., 36: 1150–1166.

Bruland, K.W., Bertine, K., Koide, M. and Goldberg, E.D., 1974. History of metal pollution in southern California coastal zone. Environ. Sci. Technol., 8: 425–432.

Bruland, K.W., Franks, R.P., Landing, W.M. and Soutar, A., 1981. Southern California inner basin sediment trap calibration. Earth Planet. Science Lett., 53: 400–432.

California Cooperative Fisheries Investigation Staff, 1989a. Physical and chemical data, CalCOFI Cruises 8801 and 8805. Scripps Inst. Oceanogr. Ref., 88-23, 80 pp.

California Cooperative Fisheries Investigation Staff, 1989b. Physical and chemical data, CalCOFI Cruises 8808, 8809, 8810. Scripps Inst. Oceanogr. Ref., 89-2, 93 pp.

California Cooperative Fisheries Investigation Staff, 1989c. Physical and chemical data, CalCOFI Cruises 8901, 8904. Scripps Inst. Oceanogr. Ref., 89-26, 88 pp.

California Cooperative Fisheries Investigation Staff, 1990. Physical and chemical data, CalCOFI Cruises 8907, 8908, 8911. Scripps Inst. Oceanogr. Ref., 90-19, 116 pp.

California Cooperative Fisheries Investigation Staff, 1991a. Physical and chemical data, CalCOFI Cruises 9003, 9004. Scripps Inst. Oceanogr. Ref., 91-4, 96 pp.

California Cooperative Fisheries Investigation Staff, 1991b. Physical and chemical data, CalCOFI Cruises 9007, 9011. Scripps Inst. Oceanogr. Ref., 91-18, 96 pp.

Calvert, S.E., 1966, Origin of diatom-rich, varved sediments from the Gulf of California. J. Geol., 74: 546–565.

Calvert, S.E., 1986. Oceanographic controls on the accumulation of organic matter in marine sediment. In: E.J. Brooks and A.J. Fleet (Editors), Marine Petroleum Source Rocks. Geol. Soc. London Spec. Publ., 26: 137–152.

Cane, M.A., 1983. Oceanographic events during El Niño. Science, 222: 1189–1195.

Cane, M.A. and Zebiak, S.E., 1985. A theory for El Niño and the Southern Oscillation. Science, 228: 1085–1087.

Christensen, C.J., 1991. An analysis of sedimentation rates and cyclicity in the laminated sediments of Santa Monica Basin, California Continental Borderland. M.S. Thesis, Univ. Southern California, Los Angeles, 144 pp. (Unpubl.)

Dean, W.E., Gardner, J.V. and Anderson, R.Y., 1991. Geochemical evidence for enhanced upwelling and organic productivity during the late Quaternary on the continental margin of northern California. In: J.J. Betancourt and V.L. Tharp (Editors), Proc. 7th Annu. Climate (PACLIM) Workshop, California Dep. Water Resour., Interagency Ecological Stud. Prog. Tech. Rep., 26: 187–203.

Doyle, L.J. and Gorsline, D.S., 1977. Marine geology of the Baja California Continental Borderland, Mexico. AAPG Bull., 61: 903–917.

Drake, D.E., Kolpack, R.L. and Fischer, P.J., 1972. Sediment transport on the Santa Barbara–Oxnard Shelf, Santa Barbara Channel, California. In: D.J.P. Swift, D.B. Duane and O.H. Pilkey (Editors), Shelf Sediment Transport: Process and Pattern. Dowden, Hutchinson and Ross, Stroudsburg, PA, pp. 307–331.

Dunbar, C.O. and Rogers, W., 1957. Principles of Stratigraphy. Wiley, New York, 356 pp.

Emery, K.O., 1954. Source of water in basins off Southern California. J. Mar. Res., 13: 1–21.

Emery, K.O., 1960. The Sea off Southern California. Wiley, New York, 366 pp.

Emery, K.O. and Hulsemann, J., 1962. The relationship of sediments, life and water in a marine basin. Deep-Sea Res., 8: 165–180.

Fuller, C.C., 1982. The use of $^{210}Pb$, $^{234}Th$, and $^{137}Cs$ as tracers of sedimentary processes in San Francisco Bay, California. M.S. Thesis, Univ. Southern California, Los Angeles, 251 pp. (Unpubl.)

Gardner, J.V. and Hemphill-Haley, E., 1986. Evidence for a stronger oxygen-minimum zone off central California during late Pleistocene to early Holocene. Geology, 14: 691–694.

Gorsline, D.S., 1992. The geologic setting of Santa Monica and San Pedro Basins, California Continental Borderland. Prog. Oceanogr., 30: 1–36.

Gorsline, D.S. and Emery, K.O., 1959. Turbidity-current deposits in San Pedro and Santa Monica Basins off southern California. Geol. Soc. Am. Bull., 70: 279–290.

Gorsline, D.S. and Teng, L.S.-Y., 1989. The California Continental Borderland. In: E.L. Winterer, D.M. Hussong and R.W. Decker (Editors), The Eastern Pacific Ocean and Hawaii. (The Geology of North America, N.) Geol. Soc. Am., pp. 471–487.

Grant, C.W., 1991. Distribution of bacterial mats (*Beggiatoa* spp.) in Santa Barbara Basin, California. a modern analog for organic-rich facies of the Monterey Formation. M.S. Thesis, California State Univ., Long Beach, 201 pp. (Unpubl.)

Hartmann, O. and Barnard, J.V., 1958. The benthic fauna of the deep basins off southern California. Allan Hancock Pacific Expeditions, 22, 67 pp.

Hickey, B.M., 1979. The California Current System—hypotheses and facts. Prog. Oceanogr., 8: 191–279.

Hickey, B.M., 1991. Variability in two deep coastal basins (Santa Monica and San Pedro) off southern California. J. Geophys. Res., 96: 16689–16708.

Hickey, B.M., 1992. Circulation over the Santa Monica–San Pedro Basins and shelf. Prog. Oceanogr., 30: 37–48.

Huh, C.A., Small, L.F., Niemnil, S., Finney, B.P., Hickey, B.M., Kachel, N.B., Gorsline, D.S. and Williams, P.M., 1990. Sedimentation dynamics in the Santa Monica–San Pedro Basins off Los Angeles: radiochemical, sediment trap and transmissometer studies. Cont. Shelf Res., 10: 137–164.

Huh, C.A., Zahnle, D.L., Small, L.F. and Noshkin, V.E., 1987. Budgets and behaviours of uranium and thorium series isotopes in Santa Monica Basin sediments. Geochim. Cosmochim. Acta, 51: 1743–1754.

Hulsemann, J. and Emery, K.O., 1961. Stratification in recent sediments of the Santa Barbara Basin as controlled by organisms and water characteristics. J. Geol., 69: 279–290.

Ingle, J.C., Jr., 1981. Origin of Neogene diatomites around the north Pacific rim. In: The Monterey Formation and Related Siliceous Rocks of California. SEPM Pacific Sect. Spec. Publ., pp. 159–179.

Jackson, G.A., Azam, F., Carlucci, A.F., Eppley, R.W., Williams, P.M., Finney, B., Huh, C.A., Small, L.F., Gorsline, D.S., Hickey, B.M., Jahnke, R.A., Kaplan, I.R., Venkatesan, M.I., Landry, M.R. and Wong, K.M., 1989. Elemental cycling and fluxes off Southern California. EOS, 70: 146–149, 154–155.

Koide, M., Bruland, K.W. and Goldberg, E.D., 1973. $^{228}Th$–$^{232}Th$ and $^{210}Pb$ geochronologies in marine and lake sediments. Geochim. Cosmochim. Acta, 37: 1171–1187.

Koide, M., Soutar, A. and Goldberg, E.D., 1972. Marine geochronology with $^{210}Pb$. Earth Planet. Sci. Lett., 14: 442–446.

Kraemer, S.M.C., 1986. Quaternary morphology, acoustic characteristics, and fan growth of the Conception Fan, Santa Barbara Basin, California Continental Borderland. M.S. Thesis, California State Univ., Northridge, 230 pp. (Unpubl.)

Lee, C.F., 1992. Seismic sequence stratigraphy and structural development of the southern outer portion of the California Continental Borderland. Ph.D. Dissert., Univ. Southern California, Los Angeles, 257 pp. (Unpubl.)

Malouta, D.A., 1978, Holocene sedimentation in Santa Monica Basin, California. M.S. Thesis, Univ. Southern California, Los Angeles, 146 pp. (Unpubl.)

Malouta, D.A., Gorsline, D.S. and Thornton, S.E., 1981. Processes and rates of recent (Holocene) basin filling in an active transform margin: Santa Monica Basin, California Continental Borderland. J. Sediment. Petrol., 51: 1077–1095.

Mathieu, G.G., Biscaye, P.E., Lupton, R.A. and Hammond, D.E., 1988. System for measurement of $^{222}Rn$ at low levels in natural waters. Health Physics, 55: 989–992.

Nardin, T.R., 1981. Seismic stratigraphy of Santa Monica and San Pedro Basins, California continental borderland: Late Neogene history of sedimentation and tectonics. Ph.D. Dissert., Univ. Southern California, Los Angeles, 295 pp. (Unpubl.)

Parrish, J.T., 1987. Paleo-upwelling and the distribution of organic-rich rocks. In: J. Brooks and A.J. Fleet (Editors), Marine Petroleum Source Rocks. Geol. Soc. London Spec. Publ., 26: 199–205.

Pisias, N.G., 1979. Paleooceanography of the Santa Barbara Basin during the last 8000 years. Quat. Res., 10: 366–384.

Poland, J.F., Garrett, A.A. and Sinnott, A., 1959. Geology, hydrology, and chemical character of ground waters in the Torrance–Santa Monica area, California. U.S. Geol. Surv. Water-Supply Pap., 1461, 425 pp.

Quinn, W.H., Zopf, D.O., Short, K.S. and Kuo Yang, R.T.W., 1978. Historical trends and statistics of the Southern Oscillation and El Niño, and Indonesian droughts. Fishery Bull., 76: 663–678.

Quinn, W.H., Neal, V.T. and Antunez de Mayolo, S.E., 1987. El Niño occurrences over the past four and a half centuries. J. Geophys. Res., 92: 14449–14461.

Rabalais, N.N., Turner, R.E., Wiseman, W.I., Jr. and Boesch, D.F., 1991. A brief summary of hypoxia on the northern Gulf of Mexico continental shelf. In: R.V. Tyson and T.H. Pearson (Editors), Modern and Ancient Continental Shelf Anoxia. Geol. Soc. London, Spec. Publ., 58: 35–48.

Reid, J.L., 1965. Intermediate waters of the Pacific Ocean. Johns Hopkins Univ. Oceanogr. Stud., 2, 85 pp.

Reimers, C.E. and Suess, E., 1983. Late Quaternary fluctuations in the cycling of organic matter off central Peru. In: E. Suess and J. Thiede (Editors), Coastal Upwelling, its Sediment Record, Part A: Responses of the Sedimentary Regime to Present Coastal Upwelling. Plenum, New York, pp. 497–526.

Reimers, C.E., Lange, C.B., Tabak, M. and Bernhard, J.M., 1990. Seasonal spillover and varve formation in the Santa Barbara Basin, California. Limnol. Oceanogr., 35: 1577–1585.

Reynolds, S., 1988. The fabrics of deep-sea detrital muds and mudstones: a scanning electron microscope study. Ph.D. Dissert., Univ. Southern California, Los Angeles, 169 pp. (Unpubl.)

Rhoads, D.C. and Morse, J.W., 1971. Evolutionary and ecologic significance of oxygen-deficient basins. Lethaia, 4: 413–428.

Richards, F.A. and Vaccaro, R.F., 1956. The Cariaco Trench, an anaerobic basin in the Caribbean Sea. Deep-Sea Res., 3: 214–228.

Ross, D.A. and Degens, E., 1974. Recent sediments of the Black Sea. In: E. Degens and D. Ross (Editors), The Black Sea—Geology, Chemistry and Biology. AAPG Mem., 20: 183–199.

Savrda, C.E., Bottjer, D.J. and Gorsline, D.S., 1984. Development of a comprehensive oxygen-deficient marine biofacies model: evidence from Santa Monica, San Pedro and Santa Barbara Basins, California Borderland. AAPG Bull., 68: 1179–1192.

Schwalbach, J.R. and Gorsline, D.S., 1990. Active Holocene channel extension from Hueneme Fan, Santa Monica Basin, California Continental Borderland. Abstr. Volume, 13th Int. Sedimentol. Cong. (Nottingham, UK.) Int. Assoc. Sedimentol., pp. 195–196.

Schwalbach, J.R., Gorsline, D.S. and Edwards, B.D., in review. The development of Holocene levee–channel fan systems into the basin floor environment of Santa Monica, San Pedro and Santa Cruz Basins, California Borderland. AAPG Bull.

Shepard, F.P. and Emery, K.O., 1941. Submarine topography

off the California coast: canyons and tectonic interpretations. Geol. Soc. Am. Spec. Pap., 31, 171 pp.

Sholkovitz, E.R., 1973. Interstitial water chemistry of Santa Barbara sediments. Geochim. Cosmochim. Acta, 37: 2043–2047.

Sholkovitz, E.R. and Gieskes, J.M., 1971. A physical–chemical study of the flushing of the Santa Barbara Basin. Limnol. Oceanogr., 16: 479–489.

Soutar, A. and Crill, P.A., 1977. Sedimentation and climatic patterns in the Santa Barbara Basin during the 19th and 20th Centuries. Geol. Soc. Am. Bull., 88: 1161–1172.

Teng, L.S.-Y., 1985. Seismic stratigraphic study of the California Continental Borderland basins—Structure, stratigraphy and sedimentation. Ph.D. Dissert., Univ. Southern California, Los Angeles, 197 pp. (Unpubl.)

Thornton, S.E., 1981. Holocene stratigraphy and sedimentary processes in Santa Barbara Basin: influence of tectonics, ocean circulation, climate and mass movement. Ph.D. Dissert., Univ. Southern California, Los Angeles, 351 pp. (Unpubl.)

Troxell, H.C. and others, 1942. Floods of March 1938 in southern California. U.S. Geol. Surv. Water-Supply Pap., 844.

Tyson, R.V. and Pearson, T.H., 1991. Modern and ancient continental shelf anoxia: an overview. In: R.V. Tyson and T.H. Pearson (Editors), Modern and Ancient Continental Shelf Anoxia, Geol. Soc. London, Spec. Publ., 58: 1–26.

Wolberg, J.R., 1967. Prediction Analysis. Van Nostrand, Princeton, 291 pp.